J|A|C|S
COMMUNICATIONS

Published on Web 12/04/2008

Detection of Breast Cancer Microcalcifications Using a Dual-modality SPECT/NIR Fluorescent Probe

Kumar R. Bhushan,[†] Preeti Misra,[†] Fangbing Liu,[†] Sanjeev Mathur,[†] Robert E. Lenkinski,[‡] and John V. Frangioni*[,†,‡]

Division of Hematology/Oncology, Department of Medicine and, Department of Radiology, Beth Israel Deaconess Medical Center, Harvard Medical School, Boston, Massachusetts 02215

Received September 18, 2008; E-mail: jfrangio@bidmc.harvard.edu

Nuclear imaging is an established clinical molecular imaging modality that offers good sensitivity deep in tissue. However, nuclear imaging is limited by several factors such as time-consuming data acquisition, expensive equipment, exposure to radioactivity, the need for highly skilled personnel, and relatively poor spatial resolution.[1] Optical imaging is a relatively new imaging modality that offers real-time, nonradioactive, and, depending on the technique, high-resolution imaging of fluorophores embedded in diseased tissues.[2] Of the various optical imaging techniques investigated to date, near-infrared (NIR, 700−900 nm wavelength) fluorescence-based imaging is of particular interest for noninvasive *in vivo* imaging because of the relatively low tissue absorption, scatter, and minimal autofluorescence of NIR light.[3]

NIR fluorescence has the potential to provide rapid, inexpensive, and nonradioactive population-based screening for breast cancer.[4−6] However, it is unclear whether currently available optical imaging systems have adequate sensitivity and/or resolution to identify breast pathology such as microcalcifications. In this study, we developed a critical reagent for exploring the limits of NIR fluorescence-based breast cancer diagnosis, namely, a simultaneous optical and nuclear contrast agent.

Bisphosphonates (BPs) bind avidly to hydroxyapatite (HA) bone mineral surfaces[7] and have many uses. BP-based radiotracers are used to diagnose osteoblastic bone lesions and to treat bone metastasis associated with breast cancer.[8] In addition, contrast agents (CAs) with BPs and phosphonates as the targeting group have been developed for use with nuclear imaging.[9,10] Although, our group[11−13] and others[14] have explored NIR imaging with BPs, to the best of our knowledge, no BP-based dual modality nuclear-NIR contrast agents have been reported. Dual-labeled targeting imaging agents, such as the one described herein, allow cross validation and direct comparison between nuclear (the gold-standard) and fluorescence optical imaging.

The trifunctional diagnostic agent Pam-Tc/Re-800 was synthesized in 5 chemical steps (Scheme 1), with an overall yield of 53%, from *N*-ε-*t*-Boc-L-lysine **1**, Me-Pam,[13] MAS_3, and IRDye800CW. The primary amine of compound **1** was conjugated with *N*-hydroxy succinimide ester of IRDye800CW to obtain Lys(*t*-Boc)-800CW-carboxylic acid **2**. Me-Pam reacted with activated compound **2** in the presence of HCTU and NMM to generate Lys(*t*-Boc)-800CW-Pam-Me **3**. Compound **3** was treated with trifluoroacetic acid and trimethylsilyl bromide to deprotect Boc on the primary amine and methylester group on phosphonates, respectively, to obtain Lys-800CW-Pam **5**. The final molecule Pam-Tc/Re-800 **6** was obtained by a ^{99m}Tc and Re solid-phase prelabeling strategy[15] on compound **5**. In all synthetic steps, compounds were purified and characterized by reversed phase preparative HPLC and LCMS.

Scheme 1[a]

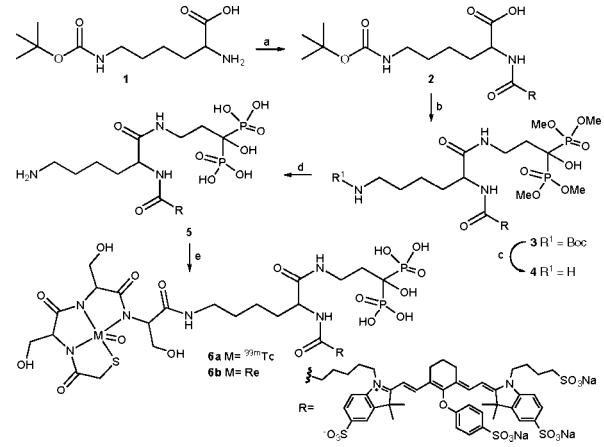

[a] Reagents and conditions: (a) IRDye800CW-NHS, DIEA, DMSO, rt, 2 h, 89%; (b) Me-Pam, HCTU, NMM, DMSO, rt, 0.5 h, 78%; (c) 95% TFA, rt, 2.5 h, 97%; (d) Me_3SiBr, DMF, rt, 12 h, and MeOH/H_2O (4:1), rt, 0.5 h, 95%; (e) ^{99m}Tc/Re-MAS_3−NHS, TEA, DMSO, rt, 1 h, 83%.

Pam-Tc/Re-800 **6** was fully characterized for its radioactivity, spectral properties (Supporting Information), and calcium salt specificity (Figure 1). The specific activity of Pam-Tc-800 **6a** was greater than or equal to 6250 Ci/mmol, and the radiochemical purity was greater than or equal to 98%. Peak absorption (781 nm) and emission (800 nm) of Pam-Re-800 **6b** are located within the "NIR window,"[16] an area of the electromagnetic spectrum that maximizes photon penetration and recovery in living tissue. The extinction coefficient of Pam-Re-800 at 781 nm was 197 000 M^{-1} cm^{-1}, and

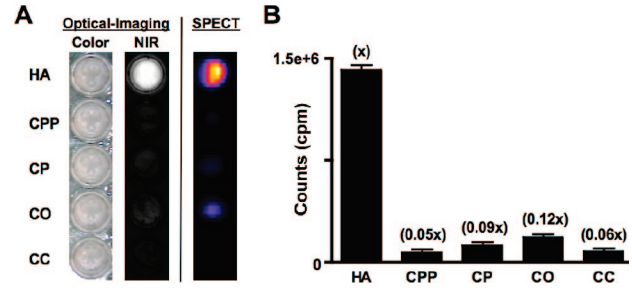

Figure 1. *In vitro* specificity of Pam-Tc/Re-800 **6** (mixture) for crystals of HA and other calcium salts. (A) Optical and SPECT images are shown. (B) Quantification (mean ± SD) of crystals from (A) using a gamma counter. All measurements (3 independent experiments) were from identically sized and shaped regions of a 96-well plate.

[†] Division of Hematology/Oncology, Department of Medicine.
[‡] Department of Radiology.

10.1021/ja807099s CCC: $40.75

its quantum yield was 8.9% in PBS. In 100% fetal bovine serum, its quantum yield was 8.7%.

To determine the selectivity and specificity of Pam-Tc/Re-800 for hydroxyapatite (HA), a major mineral component of breast cancer microcalcifications and normal bone, over other calcium salts, we incubated HA, Ca-pyrophosphate (CPP), Ca-phosphate (CP), Ca-oxalate (CO), and Ca-carbonate (CC) salts with Pam-Tc/Re-800 containing 200 nCi (^{99m}Tc) and 100 nM (Re) in 100 μL of PBS for 30 min at RT with constant motion and then washed the solutions 4 times with a 100-fold excess of PBS. SPECT/CT and NIR images were acquired for comparison. As shown in Figure 1, Pam-Tc/Re-800 **6** has a greater than 8-fold specificity for HA over other calcium salts found in the body and permits SPECT/CT and NIR fluorescence detection of HA with high sensitivity.

To help develop new screening technology, we have previously published[17] the first syngeneic rat model of breast cancer microcalcification based on ectopic expression of adenovirus-expressed bone morphogenetic protein-2 (BMP-2).

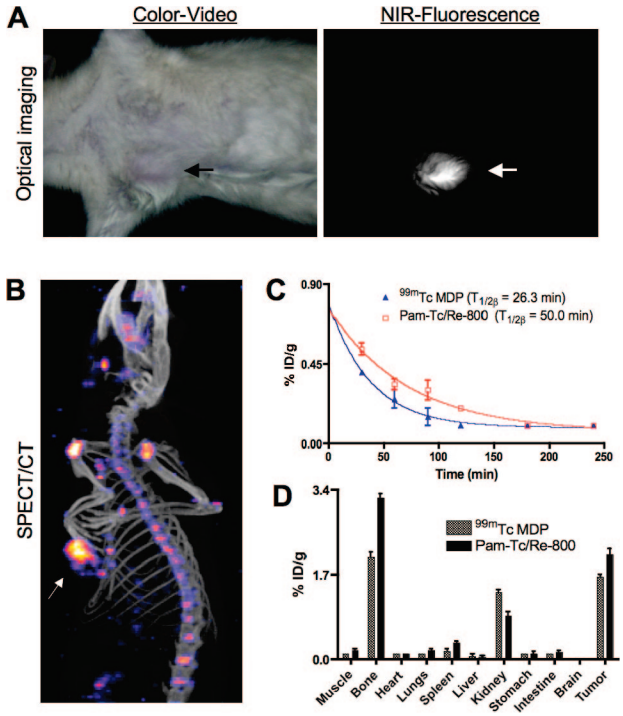

Figure 2. *In vivo* imaging of rat breast cancer microcalcification. (A) Intraoperative NIR-fluorescence imaging and (B) SPECT/CT imaging. Arrows mark location of breast cancer microcalcification. (C) Blood clearance and (D) biodistribution of Pam-Tc-800 **6a** compared to ^{99m}Tc MDP. Figure data are representative of 3 independent experiments.

This rat model of breast cancer microcalcification was used to quantify Pam-Tc/Re-800 performance *in vivo*, with intravenous injection at a dose of 500 μCi (^{99m}Tc) and 25 nmol (Re). After 4 h of clearance, simultaneous imaging of breast cancer microcalcifications was performed by both SPECT/CT and a custom intraoperative NIR fluorescence imaging system.[18] As shown in Figure 2A, breast cancer microcalcifications were observed using a simple reflectance NIR fluorescence imaging system in the presence of Pam-Re-800. Although fluorescence lifetime imaging was not explored in this study, it is possible that even higher signal-to-background ratios could be achieved with this technique. Optical detection of breast cancer microcalcification was compared to SPECT/CT. As shown in Figure 2B, Pam-Tc-800 provided high sensitivity detection of breast cancer microcalcifications as well as normal bones.

Finally, since the current gold standard for SPECT imaging of calcification is ^{99m}Tc-methylene diphosphonate (MDP), we performed a quantitative comparison of Pam-Tc-800 to ^{99m}Tc-MDP. Blood clearance $T_{1/2\beta}$ and results of biodistribution studies at 4 h post injection (p.i.) are shown in Figure 2C and 2D, respectively. The total body clearance at 4 h p.i. (70−75% ID) was almost identical for ^{99m}Tc-MDP and Pam-Tc-800; however, Pam-Tc-800 has a higher uptake in bone and tumor than ^{99m}Tc MDP. Activity that was not taken up in the tumor and bone was excreted rapidly via the kidneys into urine. In muscles and all other organs, the activity was low for both compounds. These results suggest that, in addition to use as an optical/nuclear contrast agent for validating NIR fluorescence imaging, Pam-Tc/Re-800 is itself a bone-seeking radiopharmaceutical with rapid clearance from soft tissue and slightly higher uptake in skeleton and microcalcified tumors than even ^{99m}Tc-MDP.

In conclusion, we have produced an efficient chemical synthesis of a trifunctional, HA-binding molecule, which provides simultaneous imaging by NIR fluorescence and SPECT. Quantitation by SPECT provides the "gold standard" by which NIR fluorescence tomography of breast cancer microcalcifications can now be compared and optimized.

Acknowledgment. This work was funded by NIH R01-CA-115296, NIH R01-EB-005805, high-end instrumentation Grant NIH S10-RR-023010, and grants from the Lewis Family Fund and the Ellison Foundation.

Supporting Information Available: Experimental procedures and spectroscopic data. This material is available free of charge via the Internet at http://pubs.acs.org.

References

(1) Weissleder, R.; Mahmood, U. *Radiology* **2001**, *219*, 316–33.
(2) Ntziachristos, V.; Bremer, C.; Weissleder, R. *Eur. Radiol.* **2003**, *13*, 195–208.
(3) Frangioni, J. V. *Curr. Opin. Chem. Biol.* **2003**, *7*, 626–34.
(4) Alacam, B.; Yazici, B.; Intes, X.; Nioka, S.; Chance, B. *Phys. Med. Biol.* **2008**, *53*, 837–59.
(5) Nioka, S.; Chance, B. *Technol. Cancer Res. Treat.* **2005**, *4*, 497–512.
(6) Hawrysz, D. J.; Sevick-Muraca, E. M. *Neoplasia* **2000**, *2*, 388–417.
(7) van Beek, E. R.; Lowik, C. W.; Ebetino, F. H.; Papapoulos, S. E. *Bone* **1998**, *23*, 437–42.
(8) Lipton, A.; Theriault, R. L.; Hortobagyi, G. N.; Simeone, J.; Knight, R. D.; Mellars, K.; Reitsma, D. J.; Heffernan, M.; Seaman, J. J. *Cancer* **2000**, *88*, 1082–90.
(9) Ogawa, K.; Mukai, T.; Arano, Y.; Ono, M.; Hanaoka, H.; Ishino, S.; Hashimoto, K.; Nishimura, H.; Saji, H. *Bioconjugate Chem.* **2005**, *16*, 751–7.
(10) Lam, M. G. E. H.; de Klerk, J. M. H.; van Rijk, P. P.; Zonnenberg, B. A. *Anti-Cancer Agents Med. Chem.* **2007**, *7*, 381–397.
(11) Zaheer, A.; Lenkinski, R. E.; Mahmood, A.; Jones, A. G.; Cantley, L. C.; Frangioni, J. V. *Nat. Biotechnol.* **2001**, *19*, 1148–54.
(12) Lenkinski, R. E.; Ahmed, M.; Zaheer, A.; Frangioni, J. V.; Goldberg, S. N. *Acad. Radiol.* **2003**, *10*, 1159–64.
(13) Bhushan, K. R.; Tanaka, E.; Frangioni, J. V. *Angew. Chem., Int. Ed.* **2007**, *46*, 7969–71.
(14) Zilberman, Y.; Kallai, I.; Gafni, Y.; Pelled, G.; Kossodo, S.; Yared, W.; Gazit, D. *J. Orthop. Res.* **2008**, *26*, 522–30.
(15) Misra, P.; Humblet, V.; Pannier, N.; Maison, W.; Frangioni, J. V. *J. Nucl. Med.* **2007**, *48*, 1379–89.
(16) Chance, B. *Ann. N.Y. Acad. Sci.* **1998**, *838*, 29–45.
(17) Liu, F.; Bloch, N.; Bhushan, K. R.; De Grand, A. M.; Tanaka, E.; Solazzo, S.; Mertyna, P. M.; Goldberg, S. N.; Frangioni, J. V.; Lenkinski, R. E. *Mol. Imaging* **2008**, *7*, 175–186.
(18) Tanaka, E.; Choi, H. S.; Fujii, H.; Bawendi, M. G.; Frangioni, J. V. *Ann. Surg. Oncol.* **2006**, *13*, 1671–81.

JA807099S